LETTER

doi:10.1038/nature12869

RNA viruses can hijack vertebrate microRNAs to suppress innate immunity

Derek W. Trobaugh[1], Christina L. Gardner[1], Chengqun Sun[1], Andrew D. Haddow[2], Eryu Wang[2], Elik Chapnik[3], Alexander Mildner[4], Scott C. Weaver[2], Kate D. Ryman[1] & William B. Klimstra[1]

Currently, there is little evidence for a notable role of the vertebrate microRNA (miRNA) system in the pathogenesis of RNA viruses[1]. This is primarily attributed to the ease with which these viruses mutate to disrupt recognition and growth suppression by host miRNAs[2,3]. Here we report that the haematopoietic-cell-specific miRNA miR-142-3p potently restricts the replication of the mosquito-borne North American eastern equine encephalitis virus in myeloid-lineage cells by binding to sites in the 3′ non-translated region of its RNA genome. However, by limiting myeloid cell tropism and consequent innate immunity induction, this restriction directly promotes neurologic disease manifestations characteristic of eastern equine encephalitis virus infection in humans. Furthermore, the region containing the miR-142-3p binding sites is essential for efficient virus infection of mosquito vectors. We propose that RNA viruses can adapt to use antiviral properties of vertebrate miRNAs to limit replication in particular cell types and that this restriction can lead to exacerbation of disease severity.

miRNAs are 21–23-nucleotide host-encoded RNAs that are cell-specific and bind to complementary sequences in the 3′ non-translated region (NTR) of host messenger RNAs (mRNAs)[4]. The extent of sequence complementary between the miRNA and mRNA leads to control of mRNA-encoded polypeptide levels by either a block in translation, degradation of the mRNA, or both[5,6]. For RNA viruses, limited evidence exists for host miRNAs binding to viral RNAs and restricting infection or affecting disease[1,7,8]. In the case of hepatitis C virus, the opposite is observed: the liver-specific miRNA miR-122 binds to the viral 5′ NTR, stabilizing the RNA and enhancing *in vitro* viral replication[9,10].

Wild-type North American eastern equine encephalitis virus (EEEV) strains are highly virulent mosquito-borne alphaviruses causing a 30–70% case fatality rate in humans[11]. The recognized geographic range and disease incidence of EEEV in the northeastern United States has increased over the past 10 years, raising concern about potential widespread outbreaks[12]. EEEV disease is characterized by a limited prodrome before manifestations of encephalitis, resulting from restricted myeloid cell replication and minimal induction of systemic type I interferon (IFN)[13,14]. Longer prodromes in human paediatric cases increase the likelihood of recovery, suggesting that host prodromal responses may limit disease severity[15].

Wild-type EEEV is defective for replication in human and murine macrophages and dendritic cells[13]. Using a luciferase-expressing translation reporter RNA encoding the 5′ and 3′ NTRs and translation initiation control sequences of wild-type EEEV (Extended Data Fig. 1a), we found that translation was restricted in murine RAW 264.7 (RAW) cells, a monocyte/macrophage myeloid cell line, versus BHK-21 fibroblasts (Fig. 1a and Extended Data Fig. 1d)[13]. Translation of an analogous reporter RNA derived from the related myeloid-cell-tropic wild-type Venezuelan equine encephalitis virus (VEEV) was efficient in both RAW (Fig. 1a) and BHK-21 (Extended Data Fig. 2a, b) cells[13,16]. Removal of the EEEV 5′ NTR (EEEV 5′Δ NTR) (Extended Data Fig. 1b) did not alleviate the restriction in translation in RAW cells (Fig. 1a), suggesting that the EEEV 3′ NTR confers this restriction. Indeed, transfer of the EEEV 3′ NTR to a host mRNA mimic (5′ host 3′ EEEV) (Extended Data Fig. 1c) resulted in translation blockade in RAW cells but not in BHK-21 cells (Fig. 1a and Extended Data Fig. 1d). Transfer of the VEEV 3′ NTR to the host mimic had no effect on translation in RAW or BHK-21 cells (Extended Data Fig. 2a, b). Therefore, the EEEV 3′ NTR but not the VEEV 3′ NTR contains the restricting element(s).

Two miRNA prediction algorithms, miRANDA[17] and PITA[18], identified three putative canonical and one non-canonical binding sites for the haematopoietic-cell-specific miRNA miR-142-3p in the 3′ NTR of the North American EEEV strain FL93-939 (Extended Data Fig. 3a, b). The three canonical miR-142-3p seed sites are conserved in 17 out of 23 sequenced North American EEEV strains collected between 1954 and 2012, suggesting a strong selection for their retention[19] (S.C.W., unpublished observations). To determine whether the miR-142-3p binding sites in the EEEV 3′ NTR restrict viral replication, we generated an EEEV mutant (11337) with a deletion of 260 nucleotides encompassing all of the miR-142-3p binding sites (Extended Data Fig. 3c). In BHK-21 cells, we observed no significant difference in viral replication at 12 h post-infection (h.p.i.) with 11337 compared to wild-type EEEV ($P > 0.2$, Extended Data Fig. 3d). However, replication of 11337 in RAW cells (Fig. 1b) was nearly 1,000-fold higher than wild-type EEEV within 8 h.p.i. A similar phenotype was observed after infection of human K562 and THP-1 monocyte/macrophage cells with wild-type EEEV and 11337 (Extended Data Fig. 4a, b) as well as infection of primary bone-marrow-derived dendritic cells (BMDCs), reported to express high levels of miR-142-3p[20] (Fig. 1c). Wild-type EEEV remained replication-defective in BMDCs in the absence of type I IFN signalling (Extended Data Fig. 4c)[13]; however, replication of 11337 increased, indicating that myeloid cell restriction of wild-type EEEV is IFN-independent but dependent upon the 3′ NTR sequences containing the miR-142-3p binding sites. All monocyte/macrophage cells used in this study expressed high levels of miR-142-3p in contrast to BHK-21 cells, in which miR-142-3p expression was undetectable (Extended Data Fig. 5).

To confirm a specific role for miR-142-3p in restricting EEEV replication, we expressed miR-142 in BHK-21 cells and assessed its effects on infection by wild-type EEEV, 11337 and wild-type VEEV. Ectopic expression of miR-142 in BHK-21 cells (Extended Data Fig. 5) completely blocked wild-type EEEV infection in comparison to control cells expressing a neuron-specific miRNA, miR-124 (Fig. 1d)[21]. By contrast, both 11337 and wild-type VEEV infected miR-142-expressing BHK-21 cells. To demonstrate the dependence of this restriction on the specific miR-142-3p binding sites, we generated mutant viruses that had either each of the miR-142-3p binding sequences deleted (142del) or three point mutations in each miR-142-3p binding site seed sequence (142pm; Extended Data Fig. 6a, b). These viruses replicated equally well in BHK-21 (Extended Data Fig. 6c) and RAW (Fig. 1e) cells, similar to 11337. To confirm that the increase in replication in myeloid cells was due to

[1]Center for Vaccine Research and Department of Microbiology and Molecular Genetics, University of Pittsburgh, Pittsburgh, Pennsylvania 15261, USA. [2]Institute for Human Infections and Immunity, Center for Biodefense and Emerging Infectious Diseases, and Department of Pathology, University of Texas Medical Branch, Galveston, Texas 77555, USA. [3]Department of Molecular Genetics, Weizmann Institute of Science, Rehovot 7610001, Israel. [4]Department of Immunology, Weizmann Institute of Science, Rehovot 7610001, Israel.

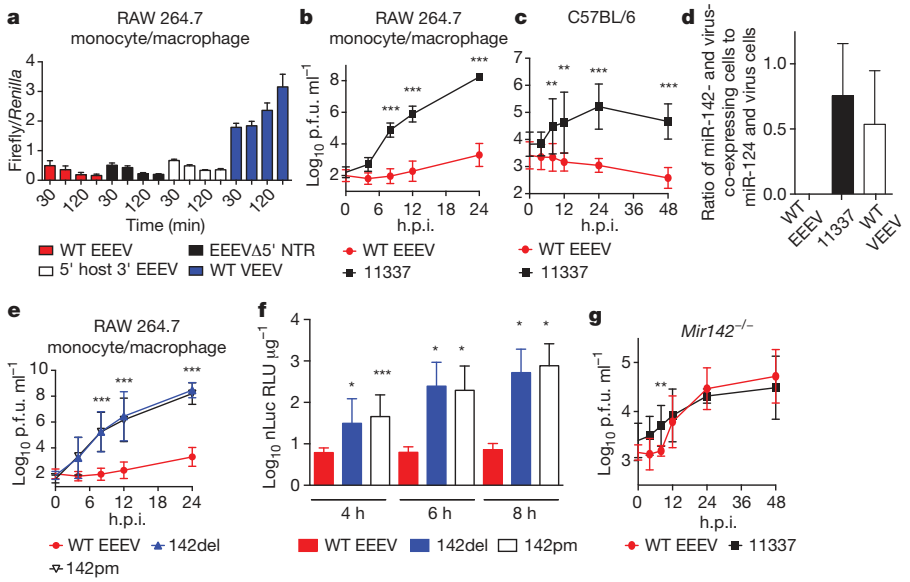

Figure 1 | EEEV restriction in myeloid cells is due to miR-142-3p binding sites in the 3′ NTR. **a**, The EEEV 3′ NTR restricts translation in RAW cells. Errors bars represent mean ± standard deviation (s.d.) from three independent experiments. WT, wild type. **b**, **c**, Replication of wild-type EEEV and 11337 in RAW cells (**b**) and C57BL/6 BMDCs (**c**). p.f.u., plaque-forming units. **d**, Overexpression of miR-142-3p in BHK-21 cells blocks EEEV infection compared to overexpression of the control miR-124. Data are represented as the ratio of the percentage of cells co-expressing the microRNA miR-142 (eGFP) and virus-infected (mCherry) to cells co-expressing miR-124 and virus-infected. Data are averaged (mean ± s.d.) from two independent experiments. **e**, Replication of EEEV 142del and 142pm in RAW cells. **f**, Ablation of the miR-142-3p binding sites in EEEV increases translation in RAW cells. nLuc, NanoLuc-luciferase; RLU, relative light units. **g**, Replication of wild-type EEEV and 11337 are similar in *Mir142*$^{-/-}$ BMDCs. Data represent the geometric mean ± s.d. from three independent experiments unless indicated. Asterisks indicate differences that are statistically significant (*$P < 0.05$, **$P < 0.01$, ***$P < 0.001$).

translation of the viral genome, we infected RAW cells with nsP3 reporter viruses to measure translation of virus-particle-delivered genomes[13]. Translation was significantly increased by 4 h.p.i. with 142del and 142pm viruses compared to wild-type EEEV (Fig. 1f). Finally, we infected BMDCs derived from miR-142-deficient (*Mir142*$^{-/-}$) mice[20] with wild-type EEEV or 11337, and detected no significant difference in viral titres between the viruses after 12 h.p.i. ($P > 0.1$, Fig. 1g). These data demonstrate that the presence of haematopoietic-cell-specific miR-142-3p binding sites in the wild-type EEEV 3′ NTR results in potent blockade of viral translation and subsequent replication in miR-142-3p-expressing cells *in vitro*.

Wild-type-EEEV-infected mice exhibit a minimal prodrome (for example, ruffled fur, hunched posture, weight loss), which is probably due to restricted myeloid cell replication and minimal type I IFN induction[13,14]. To assess the contribution of the miR-142-3p binding sites in EEEV to this phenotype, we infected CD-1 mice with wild-type EEEV or 11337. Survival times were extended in 11337-infected mice compared to wild-type-infected mice (Fig. 2a) with evidence of prodromal disease developing only in 11337-infected mice (Fig. 2b). Wild-type EEEV naturally binds heparan sulphate, which limits viral dissemination while also increasing neurovirulence[14]. Therefore, we included a heparan-sulphate-binding-defective EEEV mutant (71–77) for a comparison with wild-type VEEV, which does not bind heparan sulphate efficiently[14,22]. The 71–77 mutant was significantly attenuated compared to wild-type EEEV, and elicited signs of prodrome similar to 11337, suggesting that both heparan sulphate binding and miRNA restriction contribute to the inhibition of prodromal disease. Combining the heparan-sulphate-binding-defective mutation with the 11337 deletion (71–77/11337) increased both survival times and prodromal signs compared to wild-type EEEV or 11337 infection. The timing of prodrome onset following 71–77/11337 infection was only slightly delayed compared to wild-type-VEEV-infected mice (Fig. 2b). Consistent with limited prodrome, systemic type I IFN induction is rarely detected during wild-type EEEV infection (Fig. 2c)[13]. However, IFN-α/β was detected by 12 h.p.i. in sera from 11337-infected mice, similar to mice infected with the heparan sulphate binding mutant 71–77, and both were significantly higher than wild-type EEEV. Infection with 71–77/11337 elicited higher levels of IFN-α/β within 8 h.p.i. compared to wild-type EEEV, and at 12 h.p.i. induced IFN-α/β levels similar to those in sera from wild-type-VEEV-infected mice. These results are consistent with a study in which the addition of artificial miR-142-3p binding sites into the genome of influenza virus reduced IFN-α/β induction *in vivo*, suggesting that myeloid cell replication may be necessary for serum IFN-α/β induction with multiple viruses[23].

Previously, we observed that serum levels of IFN-α/β and prodromal signs were associated with alphavirus replication in myeloid cells within popliteal lymph nodes (PLN) after footpad inoculation[13,14]. Although wild-type EEEV replicated poorly in the PLN compared to wild-type VEEV throughout infection (Fig. 2d), both 71–77 and 11337 viruses replicated significantly more than wild-type EEEV by 12 h.p.i.. The double mutant, 71–77/11337, replicated more efficiently in PLNs at all time points compared to either 71–77 or 11337, and at levels comparable to, but lower than, those seen in wild-type-VEEV-infected PLNs. Replication restriction was alleviated for 71–77 and 71–77/11337 in type I IFN receptor-deficient *Ifnar1*$^{-/-}$ mice (Fig. 2d), and survival times for the four viruses were essentially identical ($P > 0.1$; Extended Data Fig. 7), indicating that IFN-α/β is the primary attenuating factor for 11337 and 71–77/11337, and that the 11337 mutation does not compromise replication *in vivo* in comparison with the wild-type virus. Fluorescence microscopy and flow cytometric analysis (FCA) of PLNs from mice infected with mCherry-expressing viruses demonstrated that the number of cells infected after wild-type EEEV infection were not significantly different from uninfected mice, but 11337 and 71–77/11337 infected a significantly higher number of cells compared to wild-type EEEV, with the number of cells infected with 71–77/11337 approaching those seen after wild-type VEEV infection (Fig. 2e, f). Cells infected by 11337, 71–77/11337 and wild-type VEEV were predominantly CD11b^{+} with a subset also CD11c^{+}, indicative of myeloid lineage cells (Extended Data Fig. 8). 71–77 appeared to infect some PLN cells by microscopy (Fig. 2e); however, failure to detect 71–77 PLN infection by

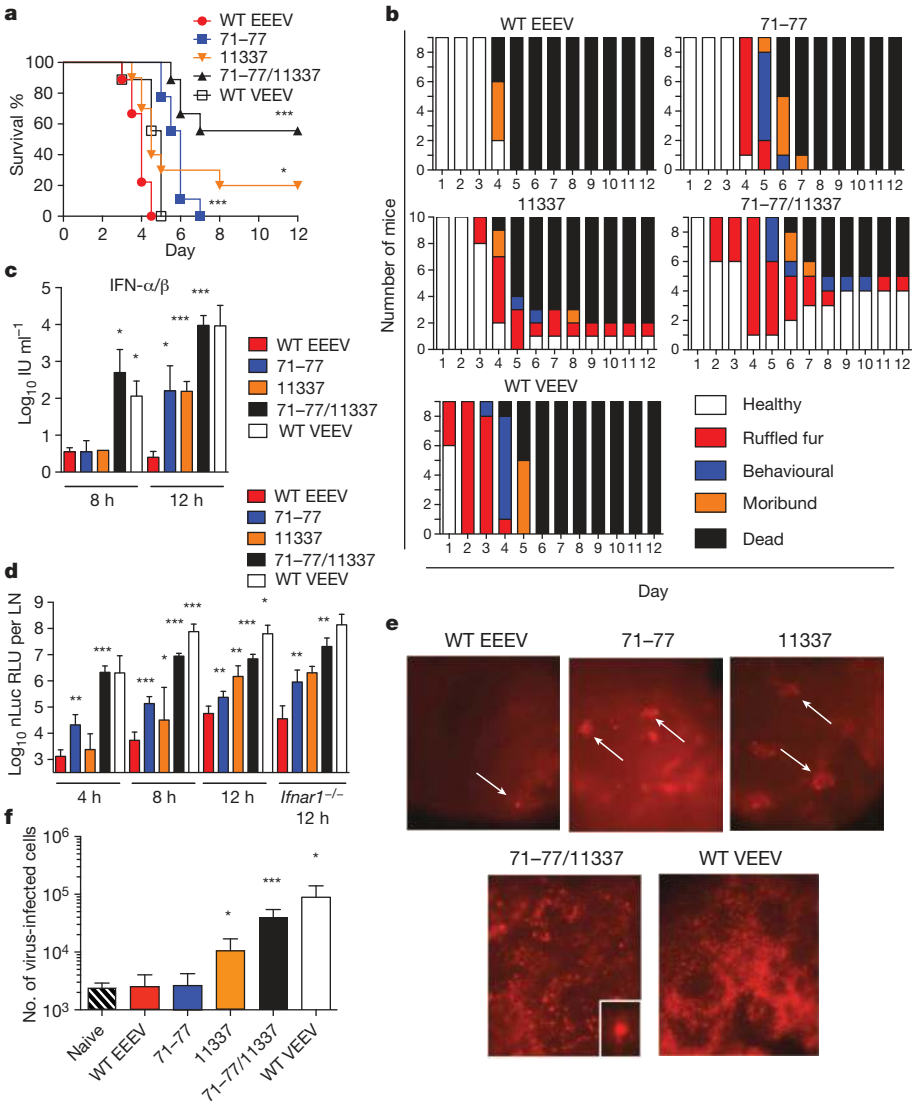

Figure 2 | miR-142-3p binding sites in EEEV 3′ NTR decrease virus replication in the lymph node and enhance disease progression. **a**, Survival curves of CD-1 mice. $n = 9$ and 10 (11337) mice per group, three independent experiments. **b**, Mice were monitored daily for clinical signs of disease. *Y*-axis represents number of mice exhibiting each sign of disease on each day. **c**, Serum levels of IFN-α/β in infected CD-1 mice. $n = 8$ mice, two independent experiments. Limit of detection of IFN-α/β ranged from 1.9 international units (IU) ml^{-1} to 3.9 IU ml^{-1}. **d**, Quantification of viral replication in the PLNs using nLuc-reporter viruses. $n = 8$ mice (CD-1) and 6 mice (*Ifnar1*$^{-/-}$) per time point, two independent experiments. **e**, Visualization of mCherry-reporter-virus-infected whole PLN from CD-1 mice 12 h.p.i. Images are representative of one PLN from two mice. Arrows indicates virus-infected cell(s) in wild-type-EEEV-, 71–77- and 11337-infected PLNs. **f**, Quantification of virus-infected cells in PLN collected 12 h.p.i. $n = 4$ (naive), 5 (71–77) or 6 (71–77/11337) mice, two independent experiments. Error bars for all experiments represent geometric mean ± s.d. Asterisks indicate differences for all experiments that are statistically significant (*$P < 0.05$, **$P < 0.01$, ***$P < 0.001$).

FCA (Fig. 2f) is consistent with the presence of miR-142-3p binding sites in the 3′ NTR of this virus. Overall, deletion of the miR-142-3p binding sites alone or in combination with disruption of the heparan-sulphate-binding ability of EEEV increased infection of PLN myeloid-lineage cells, prodromal disease signs, and type I IFN production but decreased virulence *in vivo* dependent upon a functioning IFN-α/β response.

Given the rapid mutation rate of RNA viruses, we proposed that the miR-142-3p binding sites in the EEEV 3′ NTR are maintained through positive selection during the mosquito–vertebrate transmission cycle. In C6/36 mosquito cells, the replication of 11337, 142del and 142pm viruses was significantly reduced compared to wild-type EEEV at 12 h.p.i (Fig. 3a); however, by 24 h.p.i, only the 11337 and 142del viruses remained attenuated. Furthermore, reduced infection rates of the EEEV bridge vector, *Ochlerotatus taeniorhynchus* (also known as *Aedes taeniorhynchus*)[24], via artificial blood meals were observed for 11337, 142del and 142pm viruses compared to wild-type EEEV (Fig. 3b). Therefore, specific sequences of the miR-142-3p binding sites are required for efficient mosquito infection.

We have demonstrated that host miRNA restriction of EEEV replication in myeloid cells is a novel mechanism that determines virus tropism for this cell lineage. Moreover, at least portions of these NTR sequences promote mosquito vector infection, suggesting positive selection as a mechanism for binding-site retention during natural EEEV transmission. It is also clear from these data that, at the organism level,

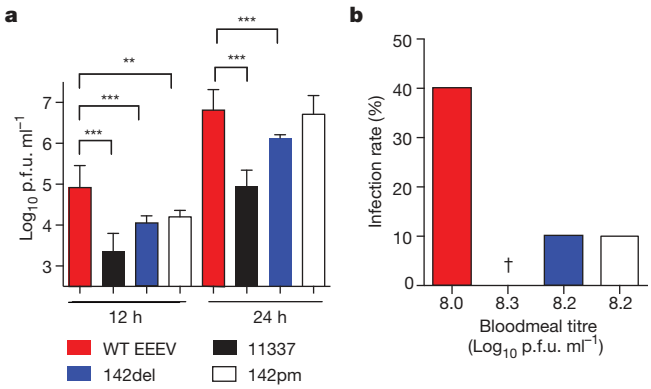

Figure 3 | EEEV sequences containing the miR-142-3p binding sites in EEEV are required for efficient mosquito infection. **a**, Replication of wild-type EEEV, 11337, 142del and 142pm in C6/36 mosquito cells. $n = 3$ or 4 (11337) independent experiments. Error bars represent geometric mean ± s.d. and asterisks indicate differences that are statistically significant using a two-tailed unpaired *t*-test comparing wild-type EEEV to all other viruses (** $P < 0.01$, ***$P < 0.001$). **b**, Infection rates of *Aedes taeniorhynchus* after ingestion of infectious bloodmeals ($n = 20$ mosquitoes per virus). † indicates 0 of 20 mosquitoes infected.

miRNA-mediated restriction of virus replication can lead to suppression of innate immune responses and exacerbation of disease, thereby benefiting the infecting microorganism. Understanding the role of miRNA expression levels and virus genotype in the efficiency of restriction may provide insight into temporal, geographical and individual host variation in EEEV and potentially other RNA virus diseases.

METHODS SUMMARY

Culture of BHK-21, L929 fibroblasts and RAW monocyte/macrophage cells and BMDCs from CD-1, *Ifnar1*$^{-/-}$ and *Mir142*$^{-/-}$ mice has been described[13,20]. Virus growth curves with BHK-21 cell titration of progeny viruses were performed as described previously[13] using enhanced GFP (eGFP) or mCherry reporter viruses described below.

Wild-type EEEV, wild-type VEEV and host mimic luciferase-expressing translation reporters were described previously[25,26]. Other reporters were constructed using the QuikChange II XL mutagenesis kit. Translation assays were performed as described with minor modifications[13].

Construction of cDNA clones of VEEV ZPC 738 (ref. 27; wild-type VEEV), EEEV FL93-939 (ref. 28; wild-type EEEV) and EEEV 71–77 (ref. 14) were described previously. The EEEV 11337, 142del and 142pm mutants were constructed from the FL93-939 cDNA. mCherry-, eGFP- and nLuc-expressing versions of all viruses were constructed similarly to a described capsid-PE2 fusion reporter viruses using the QuikChange II XL kit[29].

The eGFP-expressing pCMV-miR-142 or pCMV-miR-124 expression plasmids were electroporated into BHK-21 cells. After ~18 h, cells were infected with mCherry reporter viruses for 8 h followed by assessment of co-expression of the miRNA (eGFP) and virus reporter (mCherry) using fluorescence microscopy.

Outbred CD-1 mice were infected subcutaneously and evaluated for morbidity and mortality as described[13,14]. For tissues, CD-1 or *Ifnar1*$^{-/-}$ mice were infected with nLuc or mCherry reporter viruses. PLNs were collected at indicated time points and processed for Nano-Glo luciferase assay, for fluorescence microscopy, or for FCA of virus-infected cells. Serum IFN-α/β was measured using a standard biological assay as described[13].

Adult female *A. taeniorhynchus* mosquitoes were infected with EEEV viruses in artificial blood meals. Engorged females were incubated 10 days and assayed for infection by infection of Vero cells and observation for cytopathic effects[30].

Online Content Any additional Methods, Extended Data display items and Source Data are available in the online version of the paper; references unique to these sections appear only in the online paper.

Received 31 July; accepted 5 November 2013.
Published online 18 December 2013.

1. Cullen, B. R. MicroRNAs as mediators of viral evasion of the immune system. *Nature Immunol.* **14,** 205–210 (2013).
2. Pham, A. M., Langlois, R. A. & tenOever, B. R. Replication in cells of hematopoietic origin is necessary for Dengue virus dissemination. *PLoS Pathog.* **8,** e1002465 (2012).
3. Zheng, Z. *et al.* Human microRNA hsa-miR-296–5p suppresses enterovirus 71 replication by targeting the viral genome. *J. Virol.* **87,** 5645–5656 (2013).
4. Bartel, D. P. MicroRNAs: target recognition and regulatory functions. *Cell* **136,** 215–233 (2009).
5. Doench, J. G. & Sharp, P. A. Specificity of microRNA target selection in translational repression. *Genes Dev.* **18,** 504–511 (2004).
6. Djuranovic, S., Nahvi, A. & Green, R. miRNA-mediated gene silencing by translational repression followed by mRNA deadenylation and decay. *Science* **336,** 237–240 (2012).
7. Otsuka, M. *et al.* Hypersusceptibility to vesicular stomatitis virus infection in Dicer1-deficient mice is due to impaired miR24 and miR93 expression. *Immunity* **27,** 123–134 (2007).
8. Lecellier, C. H. *et al.* A cellular microRNA mediates antiviral defense in human cells. *Science* **308,** 557–560 (2005).
9. Shimakami, T. *et al.* Stabilization of hepatitis C virus RNA by an Ago2-miR-122 complex. *Proc. Natl Acad. Sci. USA* **109,** 941–946 (2012).
10. Jopling, C. L., Yi, M., Lancaster, A. M., Lemon, S. M. & Sarnow, P. Modulation of hepatitis C virus RNA abundance by a liver-specific microRNA. *Science* **309,** 1577–1581 (2005).
11. Griffin, D. E. in *Fields Virology* (ed. Knipe, D. M.) 1023–1068 (Lippincott Williams & Wilkins, 2006).
12. Armstrong, P. M. & Andreadis, T. G. Eastern equine encephalitis virus–old enemy, new threat. *N. Engl. J. Med.* **368,** 1670–1673 (2013).
13. Gardner, C. L. *et al.* Eastern and Venezuelan equine encephalitis viruses differ in their ability to infect dendritic cells and macrophages: impact of altered cell tropism on pathogenesis. *J. Virol.* **82,** 10634–10646 (2008).
14. Gardner, C. L., Ebel, G. D., Ryman, K. D. & Klimstra, W. B. Heparan sulfate binding by natural eastern equine encephalitis viruses promotes neurovirulence. *Proc. Natl Acad. Sci. USA* **108,** 16026–16031 (2011).
15. Silverman, M. A. *et al.* Eastern equine encephalitis in children, Massachusetts and New Hampshire, USA, 1970–2010. *Emerg. Infect. Dis.* **19,** 194–201 (2013).
16. MacDonald, G. H. & Johnston, R. E. Role of dendritic cell targeting in Venezuelan equine encephalitis virus pathogenesis. *J. Virol.* **74,** 914–922 (2000).
17. Enright, A. J. *et al.* MicroRNA targets in *Drosophila. Genome Biol.* **5,** R1 (2003).
18. Kertesz, M., Iovino, N., Unnerstall, U., Gaul, U. & Segal, E. The role of site accessibility in microRNA target recognition. *Nature Genet.* **39,** 1278–1284 (2007).
19. Pruitt, K. D., Tatusova, T., Brown, G. R. & Maglott, D. R. NCBI Reference Sequences (RefSeq): current status, new features and genome annotation policy. *Nucleic Acids Res.* **40,** D130–D135 (2012).
20. Mildner, A. *et al.* Mononuclear phagocyte miRNome analysis identifies miR-142 as critical regulator of murine dendritic cell homeostasis. *Blood* **121,** 1016–1027 (2013).
21. Lagos-Quintana, M. *et al.* Identification of tissue-specific microRNAs from mouse. *Curr. Biol.* **12,** 735–739 (2002).
22. Bernard, K. A., Klimstra, W. B. & Johnston, R. E. Mutations in the E2 glycoprotein of Venezuelan equine encephalitis virus confer heparan sulfate interaction, low morbidity, and rapid clearance from blood of mice. *Virology* **276,** 93–103 (2000).
23. Langlois, R. A., Varble, A., Chua, M. A., García-Sastre, A. & tenOever, B. R. Hematopoietic-specific targeting of influenza A virus reveals replication requirements for induction of antiviral immune responses. *Proc. Natl Acad. Sci. USA* **109,** 12117–12122 (2012).
24. Scott, T. W. & Weaver, S. C. Eastern equine encephalomyelitis virus: epidemiology and evolution of mosquito transmission. *Adv. Virus Res.* **37,** 277–328 (1989).
25. Tesfay, M. Z. *et al.* Alpha/beta interferon inhibits cap-dependent translation of viral but not cellular mRNA by a PKR-Independent mechanism. *J. Virol.* **82,** 2620–2630 (2008).
26. Bick, M. J. *et al.* Expression of the zinc-finger antiviral protein inhibits alphavirus replication. *J. Virol.* **77,** 11555–11562 (2003).
27. Anishchenko, M. *et al.* Generation and characterization of closely related epizootic and enzootic infectious cDNA clones for studying interferon sensitivity and emergence mechanisms of Venezuelan equine encephalitis virus. *J. Virol.* **78,** 1–8 (2004).
28. Aguilar, P. V. *et al.* Structural and nonstructural protein genome regions of eastern equine encephalitis virus are determinants of interferon sensitivity and murine virulence. *J. Virol.* **82,** 4920–4930 (2008).
29. Thomas, J. M., Klimstra, W. B., Ryman, K. D. & Heidner, H. W. Sindbis virus vectors designed to express a foreign protein as a cleavable component of the viral structural polyprotein. *J. Virol.* **77,** 5598–5606 (2003).
30. Brault, A. C. *et al.* Venezuelan equine encephalitis emergence: enhanced vector infection from a single amino acid substitution in the envelope glycoprotein. *Proc. Natl Acad. Sci. USA* **101,** 11344–11349 (2004).

Acknowledgements We thank M. Dunn for excellent technical support, and M. Diamond for reading of the manuscript. This work was supported by National Institutes of Health (NIH) training grants AI049820-10 and AI060525-08 (D.W.T.), research grants AI083383 and AI095436 (W.B.K.) and a Project Grant (K.D.R.) from National Institute of Allergy and Infectious Diseases through the Pacific Northwest Regional Centers for Excellence in Biodefense and Emerging Infectious Diseases Research (U54 AI081680). The views expressed are those of the authors and do not necessarily represent the views of the NIH.

Author Contributions D.W.T., S.C.W., K.D.R. and W.B.K. designed the experiments and analysed the data. D.W.T., C.L.G., A.D.H. and E.W. performed the experiments. C.S., E.C. and A.M. provided key reagents. D.W.T. and W.B.K. wrote the manuscript. All authors discussed the results and commented on the manuscript.

Author Information Reprints and permissions information is available at www.nature.com/reprints. The authors declare no competing financial interests. Readers are welcome to comment on the online version of the paper. Correspondence and requests for materials should be addressed to W.B.K. (klimstra@pitt.edu).

METHODS

Cell culture. Baby hamster kidney cells (BHK-21), L929 fibroblasts and RAW 264.7 (RAW) macrophage/monocyte cells were maintained as described previously[13]. BMDCs from CD-1, *Ifnar1*$^{-/-}$ and *Mir142*$^{-/-}$ mice[20] were generated and maintained as described previously[13]. However, *Mir142*$^{-/-}$ bone marrow was collected and frozen in 10% dimethyl sulphoxide and 90% FBS before culture. *Aedes albopictus* C6/36 mosquito cells were maintained in minimum essential medium alpha medium (Cellgro) supplemented with 10% FBS and 1% L-glutamine (Gibco).

Translation reporters and dual luciferase assay. Wild-type EEEV, wild-type VEEV and host mimic luciferase-expressing translation reporters (diagram in Extended Data Fig. 1) were generated previously[25,26]. The host mimic translation reporters encode a short 5′ and 3′ NTR fused in-frame with the fLuc gene. The EEEV 5′Δ NTR and VEEV 5′Δ NTR reporters were constructed using QuikChange II XL mutagenesis kit (Agilent Technologies) and the primers listed in Extended Data Table 1. The chimaeric 5′ host 3′ EEEV and 5′ host 3′ VEEV translation reporter was constructed by addition of a restriction endonucleases site into the host fLuc mimic reporter using QuikChange II XL mutagenesis and the primers listed in Extended Data Table 1. The 3′ NTR of EEEV or VEEV was then placed into the host fLuc mimic after the fLuc gene with endonuclease digestion. Translation assays were performed as described previously with modifications[13]. Each *in vitro*-transcribed reporter RNA (7.5 μg per reaction) and the *Renilla* reporter RNA (0.75 μg per reaction) were electroporated into RAW and BHK-21 cells (6×10^6 cells per reaction) using the Neon Transfection system (Invitrogen; BHK-21: 1,200 V, 30 ms, 1 pulse; RAW: 1750 V, 25 ms, 1 pulse). Two reactions were combined and aliquoted in triplicate per time point per experiment. Firefly relative light units (RLU) data were normalized to *Renilla* RLUs in each sample.

Viruses. Construction of cDNA clones of VEEV ZPC 738 (ref. 27) (wild-type VEEV), EEEV FL93-939 (ref. 28) (wild-type EEEV) and EEEV 71–77 (ref. 14) were described previously. mCherry, eGFP and nLuc (Promega) reporter viruses were constructed as a cleavable in-frame fusion between the capsid and E3 proteins using QuikChange II XL mutagenesis kit with the first 5 amino acids of E3 fused in-frame to the amino terminus of the reporter genes and the 2A-like protease of *Thosea asigna* virus (TaV) fused to the carboxy terminus[29,31]. The EEEV 11337, 142del and 142pm mutants were generated using the EEEV FL93-939 complementary DNA clone and QuikChange mutagenesis II XL kit and primers listed in Extended Data Table 2. Wild-type EEEV nsP3–nLuc translation reporter virus was constructed with the nLuc gene fused in frame with nsP3[13,31]. The 3′ NTR of each mutant was placed into TaV and nsP3–nLuc reporter viruses using EcoRI and Not I.

Virus infections and plaque assay. Virus growth curves were performed as described previously using eGFP or mCherry reporter viruses described above[13]. In brief, BHK-21, RAW and C6/36 cells (2×10^5 cells per well) were infected in triplicate in 24-well plates at a multiplicity of infection (m.o.i.) of 0.1 p.f.u. per cell or 1 p.f.u. per cell (C6/36). BMDCs (1×10^5 cells) were infected in triplicate at a m.o.i. of 5 p.f.u. per cell in suspension, washed and transferred into 24-well plates. For growth curves, supernatant was collected at time zero and indicated time points for titration by plaque assay on BHK-21 cells. For nsP3 translation reporter assays, RAW (4×10^5 cells per well) were infected at an m.o.i. of 1 p.f.u. per cell in triplicate with nsP3–nLuc reporter viruses and collected at indicated time points using 1× Passive Lysis Buffer (PLB; Promega). nLuc expression was quantified using the Nano-Glo Luciferase assay system (Promega) according to manufacturer's guidelines and normalized to protein concentration using a Pierce BCA protein assay (Thermo Scientific).

miRNA overexpression. The pCMV-miR-142 expression plasmid and a neuron-specific miRNA, pCMV-miR-124, (OriGene) were electroporated (4 μg each) into BHK-21 cells (1×10^6 cells) using the Amaxa Nucleofector Kit L (Lonza) according to manufacturer's guidelines. After ~18 h, cells were infected with wild-type EEEV, wild-type VEEV or EEEV 11337 mCherry TaV viruses (m.o.i. = 1 p.f.u. per cell) for 8 h followed by fixation. Co-expression of the miRNA (eGFP) and virus reporter (mCherry) was determined using fluorescence microscopy as described previously[13]. Data are represented as the ratio of the percentage of cells co-expressing the microRNA, miR-142, (eGFP) and virus-infected (mCherry) to cells co-expressing miR-124 and virus-infected.

RT–PCR to detect miR-142-3p. Total cellular RNA was collected from cells using Trizol (Life Technologies) and 1-bromo-3-chloropropane and isopropanol. RNA (200 ng) was reverse transcribed with the miScript II RT kit (Qiagen) according to manufacturer's guidelines. cDNA was diluted in water and mature miR-142-3p was quantified using the miScript SYBR Green PCR kit (Qiagen) according to manufacturer's guidelines using the miR-142-3p-specific primer 5′-TGTAGTGT TTCCTACTTTATGGA-3′. miR-142-3p expression was normalized to RNU6B using the primer 5′-GATGACACGCAAATTCGTGAA-3′ and the $\Delta\Delta C_T$ method. Data are calculated as fold change in expression compared to expression of miR-142-3p in BHK-21 cells in which miR-142-3p expression was undetected.

Mouse infections, tissue collection, nLuc analysis. Six-week-old female outbred CD-1 mice (Charles River Laboratories) and 6–9-week-old female or male *Ifnar1*$^{-/-}$ mice bred in house were randomly distributed, infected subcutaneously in both footpads and scored daily for clinical signs and weight loss as described previously[13,14]. Two investigators were used to analyse the clinical symptoms observed in the mice during morbidity and mortality studies. Investigators were not privy to timing and onset of clinical symptoms from previous experiment. For tissue collection, mice were infected with 10^3 p.f.u. of nLuc- or mCherry-reporter TaV viruses. PLNs were collected at indicated time points and either frozen on dry ice, placed in 200 μl 1× PLB for nLuc analysis or placed in 4% paraformaldehyde (PFA) for 1 week for visualization on a fluorescence microscope. PLNs were homogenized and analysed for nLuc expression using the Nano-Glo Luciferase assay system. All EEEV PLNs were photographed using equal exposure times (615 ms) whereas the VEEV lymph node, owing to an increased signal, was visualized using a lower exposure time (90 ms) at ×4 magnification using cellSens Standard software (Olympus). The 71–77/11337 inset was imaged at ×40 magnification and 457-ms exposure length. Brightness and contrast of the images were adjusted equally using Adobe Photoshop CS3 and Microsoft Powerpoint software. All animal procedures were carried out in accordance with American Association for the Accreditation of Laboratory Animal Care International-approved institutional guidelines for animal care and use and approved by the University of Pittsburgh Institutional Animal Care and Use Committee. No statistical methods were used to ensure adequate power. Sample sizes were chosen based upon experience with the mortality kinetics of EEEV in mice and historical group number requirements to achieve statistical significance yet use the fewest animals possible.

Quantification of virus-infected cells from PLN. To quantify number of virus infected cells in PLNs, CD-1 mice were infected as above, collected at 12 h.p.i., minced and incubated with Liberase TL (0.2 mg ml^{-1}; Roche) and DNaseI (0.2 mg ml^{-1}; Roche) for 20 min at 37 °C. After removal of cellular debris, cells were stained with anti-mouse CD16/32 (93; eBioscience), and Fixable Viability Dye eFluor 506 (eBioscience). After washing, cells were stained with anti-mouse CD11b (clone N418, Tonbo Biosciences), and anti-mouse CD11c (M1/70; eBioscience) to identify myeloid cells. Cells were fixed in 4% PFA and analysed using a BD LSRFortessa (BD Bioscience) and FloJo Software (Tree Star). Number of virus-infected cells was calculated based on total number of cells in both PLNs per mouse.

IFN-α/β analysis. Serum IFN-α/β was measured using a standard biological assay on L929 cells as described previously[13].

Mosquito infection. Adult female *Aedes (Ochlerotatus) taeniorhynchus* mosquitoes were infected with EEEV, 11337, 142del and 142pm mCherry- or eGFP-reporter TaV viruses in artificial bloodmeals. Engorged females were incubated at 27 °C for 10 days under 12 h light/12 h dark circadian lighting conditions and assayed for infection by inoculation onto Vero cell monolayers and observation for cytopathic effects as described previously[30].

Statistical analysis. Statistical significance for mortality curves was determined by Mantel–Cox log-rank test. For all viral growth curve experiments, data was $\log_{10}$ transformed and unpaired *t*-tests were performed and corrected for multiple comparisons using the Holm–Sidak method with alpha = 0.05. For all other experiments, a two-tailed unpaired *t*-test was used (GraphPad Prism software). Statistical analysis for nLuc expression in CD-1 PLN was performed comparing wild-type EEEV versus the other EEE viruses whereas wild-type VEEV was compared to only 71–77/11337 at each time point. nLuc expression in *Ifnar1*$^{-/-}$ mice was compared to the corresponding viruses at 12 h.p.i. in CD-1 mice only. Statistical analysis for quantification of the number of infected cells in PLN was performed between the EEEV mutant viruses and wild-type EEEV, and between wild-type VEEV and 71–77/11337.

31. Sun, C., Gardner, C. L., Watson, A. M., Ryman, K. D. & Klimstra, W. B. Stable, high-level expression of reporter proteins from improved alphavirus expression vectors to track replication and dissemination during encephalitic and arthritogenic disease. *J. Virol.* (http://dx.doi.org/10.1128/JVI.02990-13) (4 December 2013).

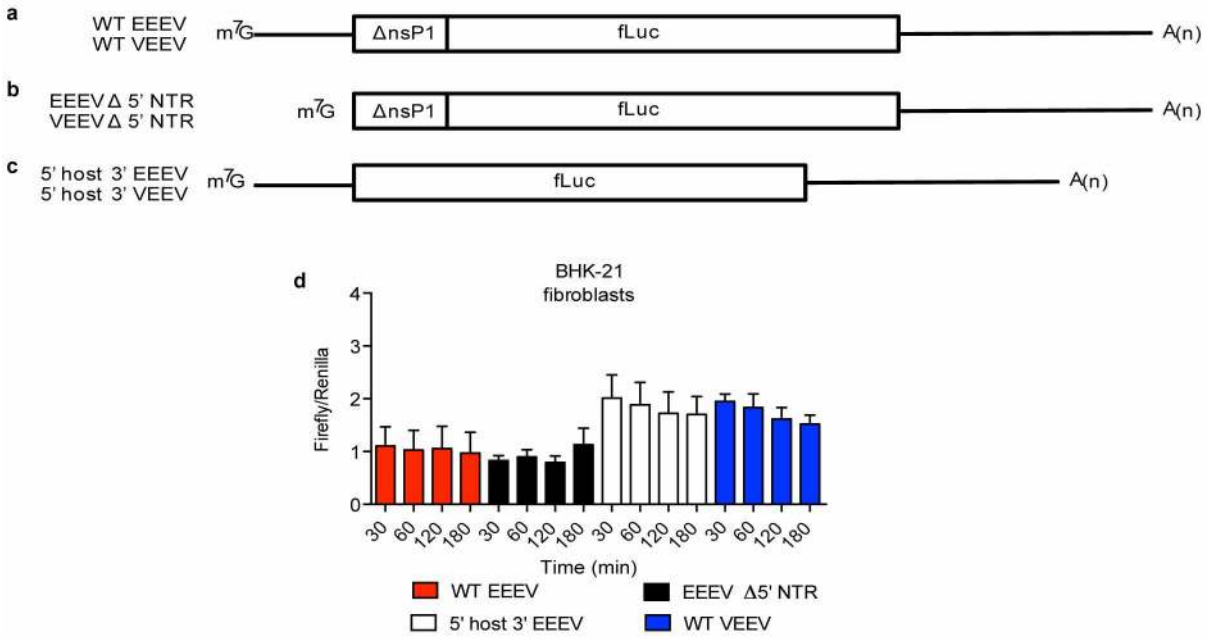

Extended Data Figure 1 | EEEV 3′ NTR does not restrict translation in BHK-21 fibroblasts. **a**, Wild-type EEEV and wild-type VEEV translation reporters encode the translational initiation control sequences fused to the Firefly luciferase (fLuc) gene. **b**, The EEEV 5′Δ NTR and VEEV 5′Δ NTR encode the truncated nsP1 gene and only the 3′ NTR of either EEEV or VEEV, respectively. **c**, The 3′ NTR of EEEV or VEEV was inserted into a host mRNA mimic reporter to generate the 5′ host 3′ EEEV or 5′ host 3′ VEEV reporters. All translation reporters contain a 5′ cap and a 3′ poly(A) tail. **d**, Translation of wild-type EEEV, EEEV 5′Δ NTR, and 5′ host 3′ EEEV reporters in BHK-21 cells. Error bars represent mean ± s.d. and the data are averaged from three independent experiments performed in triplicate. WT, wild type.

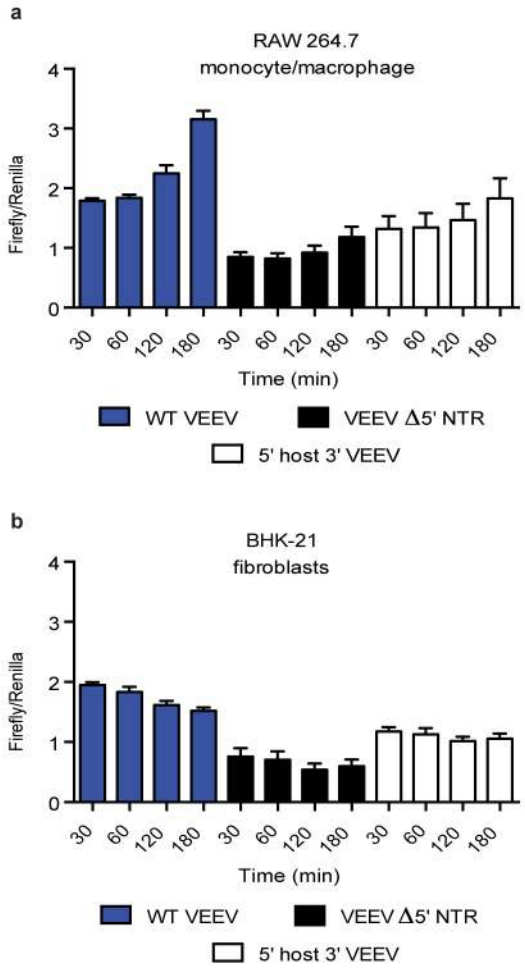

Extended Data Figure 2 | VEEV 3′ NTR does not restrict translation in myeloid cells. **a**, **b**, Translation of wild-type VEEV, VEEV 5′Δ NTR, and 5′ host 3′ VEEV reporters in RAW (**a**) and BHK-21 (**b**) cells. Error bars represent mean ± s.d. and the data are averaged from three independent experiments performed in triplicate.

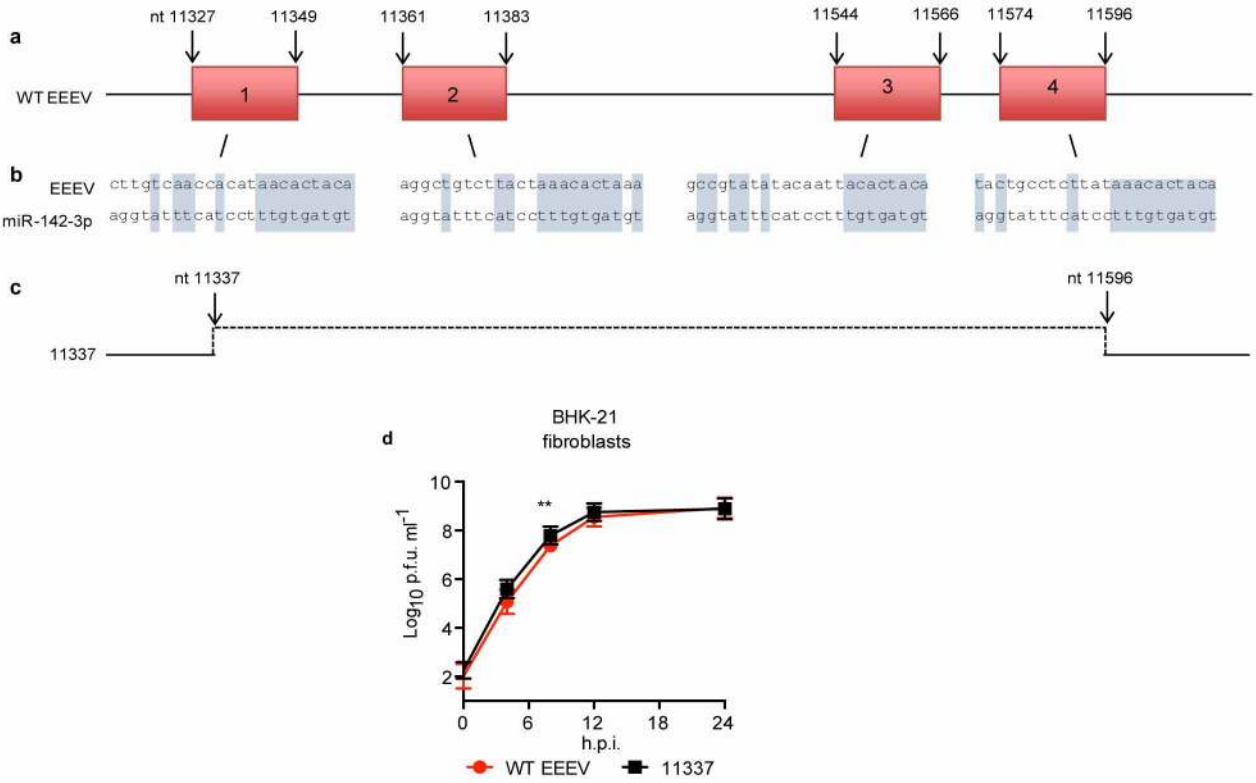

Extended Data Figure 3 | Removal of miR-142-3p binding sites in the 3′NTR of EEEV does not alter replication in BHK-21 fibroblasts. **a**, Red boxes indicate the four miR-142-3p binding sites in the 3′ NTR. Numbers represent nucleotide (nt) positions at the start and end of each miRNA binding site. **b**, Grey boxes correspond to the complimentary nts in the EEEV 3′ NTR and miR-142-3p. **c**, EEEV mutant 11337 contains a deletion in the 3′ NTR from nt 11,337 to 11,596. **d**, Replication of wild-type EEEV and 11337 in BHK-21 cells. $n = 3$ independent experiments. Error bars indicate geometric mean ± s.d., and asterisks indicate differences that are statistically significant ($^{**}P < 0.01$).

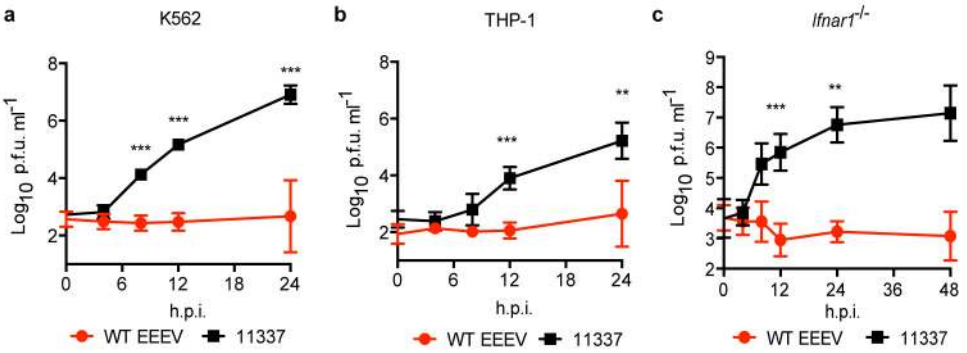

Extended Data Figure 4 | miR-142-3p binding sites in EEEV restrict replication in human macrophage/monocyte cell lines and primary murine *Ifnar1*$^{-/-}$ BMDCs. **a**, **b**, Replication of wild-type EEEV and 11337 in human K562 (**a**) and THP-1 (**b**) cells. $n = 2$ (THP-1) and 3 (K562) independent experiments. **c**, Removal of type I IFN does not alleviate wild-type EEEV restriction in primary murine *Ifnar1*$^{-/-}$ BMDCs. n = three independent experiments. Data represent the geometric mean ± s.d., and asterisks indicate differences that are statistically significant (*$P < 0.05$, **$P < 0.01$, ***$P < 0.001$).

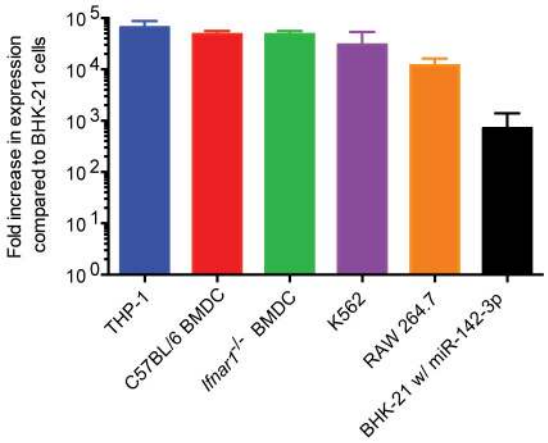

Extended Data Figure 5 | Relative expression of miR-142-3p in mouse and human cells. Quantitative RT–PCR on primary murine BMDCs, murine and human monocyte/macrophage cell lines, and BHK-21 cells expressing miR-142-3p (BHK-21 w/miR-142-3p). Fold increase in expression is calculated compared to expression of miR-142-3p in BHK-21 cells in which miR-142-3p expression was undetectable.

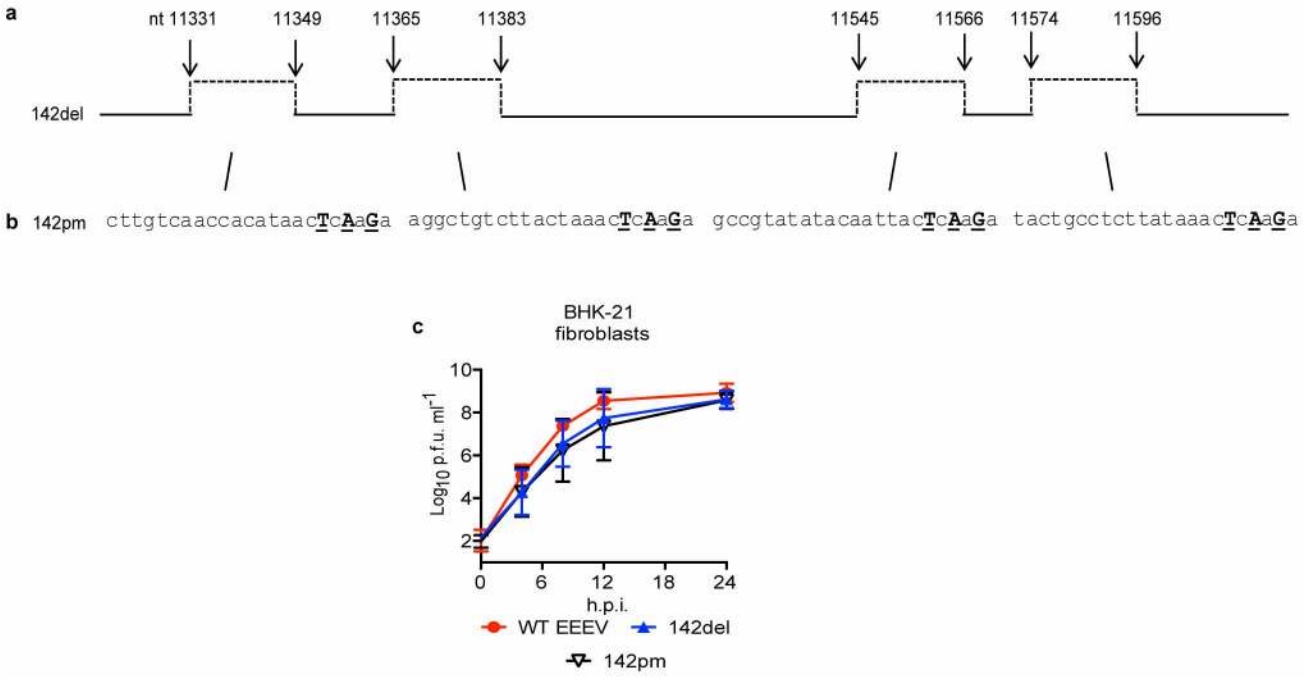

Extended Data Figure 6 | Specific deletion of the miR-142-3p binding sites in the 3′ NTR of wild-type EEEV does not alter replication in BHK-21 fibroblasts. **a**, EEEV 142del virus contains four deletions corresponding to the complimentary nucleotides in the 3′ NTR that bind to miR-142-3p, eliminating all four miR-142-3p binding sites. **b**, EEEV 142pm virus contains three point mutations in each of the miR-142-3p binding sites that correspond to the seed sequence of miR-142-3p. **c**, Replication of wild-type EEEV and 11337 in BHK-21 cells. n = three independent experiments. Error bars indicate geometric mean ± s.d.

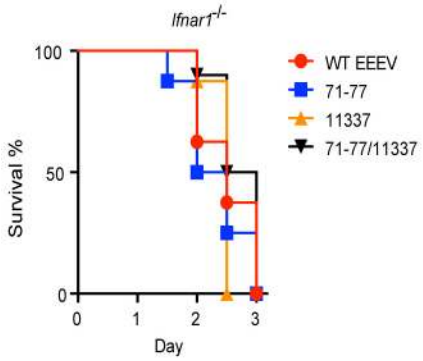

Extended Data Figure 7 | Type I IFN attenuates 11337 and 71–77/11337. Survival curves in *Ifnar1*$^{-/-}$ mice. $n = 8$ and 10 (71–77/11337) mice per virus from two independent experiments.

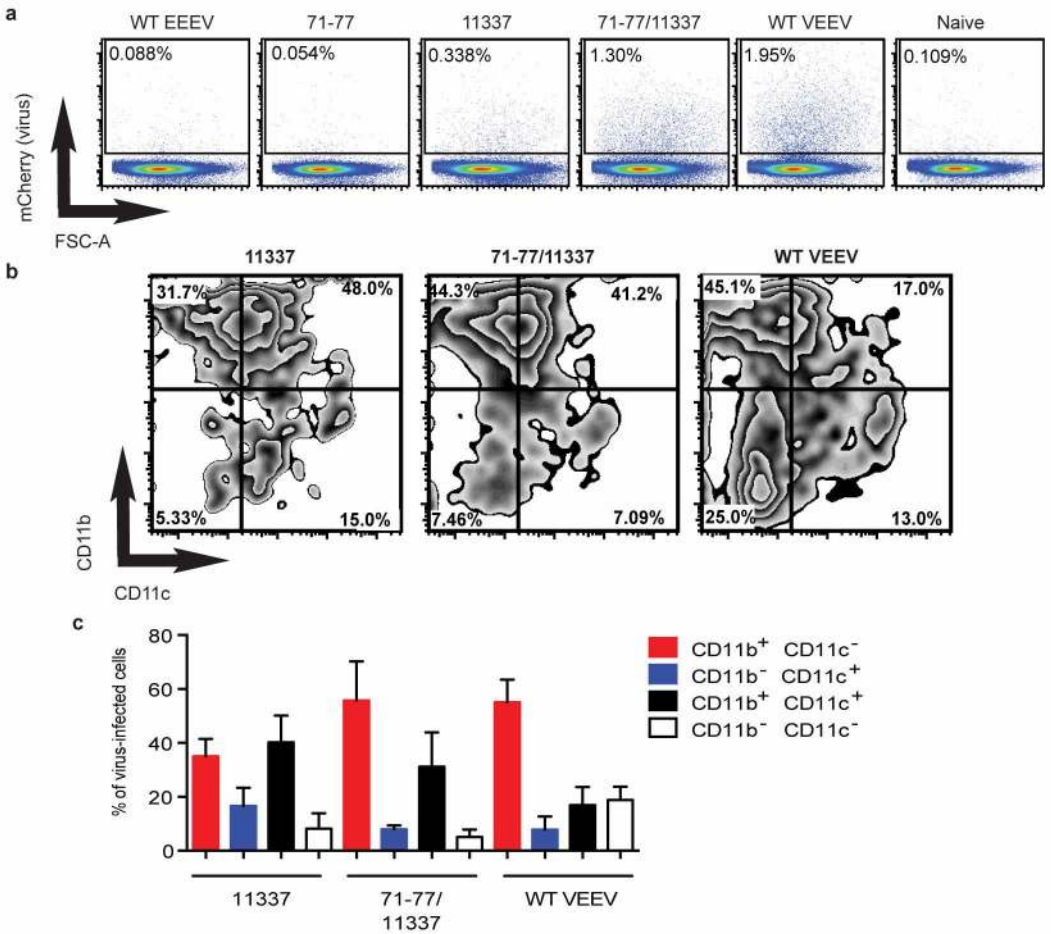

Extended Data Figure 8 | EEEV 11337 and 71–77/11337 infect myeloid lineage cells in the PLN. **a**, Per cent virus-infected cells in PLN in naïve, wild-type VEEV-, wild-type EEEV-, 71–77-, 11337- and 71–77/11337-infected mice. Plots are representative of $n = 4$ (naive), 5 (71–77) or 6 (71–77/11337) mice from two independent experiments. **b**, **c**, Wild-type VEEV, 11337 and 71–77/11337 infect myeloid lineage cells in the PLN. **b**, Representative flow plot from 1 mouse of CD11b (*y*-axis) and CD11c (*x*-axis) expression on virus-infected cells. $n = 4$ (naïve), 5 (71–77) or 6 (71–77/11337) mice from two independent experiments. **c**, Summary of CD11b and CD11c expression on virus-infected cells from wild-type VEEV-, 11337- and 71–77/11337-infected PLNs. Only mice with responses above naive mice background levels were used to determine CD11b and CD11c expression.

Extended Data Table 1 | Primers used to generate the translation reporters using the QuikChange II XL mutagenesis kit

Reporter	Primer Name	Sequence
EEEV Δ5′ NTR	EEEV Δ5′ NTR-F	5'-agctcggatcctaatacgactcactatagatggagaaagttcatgttgacttagacgca-3'
	EEEV Δ5′ NTR-R	5'-tgcgtctaagtcaacatgaactttctccatctatagtgagtcgtattaggatccgagct-3'
VEEV Δ5′ NTR	VEEV Δ5′ NTR-F	5'-agaggatccctaatacgactcactatagatggagaaagttcacgttgacatcgaggaa-3'
	VEEV Δ5′ NTR-R	5'-ttcctcgatgtcaacgtgaactttctccatctatagtgagtcgtattagggatcctct-3'
Host mimic w/Not1	fLuc-Not1-F	5'-cccaaaaaaaaaaaaaaaaaaaaaaaaaaaaagcggccgccgtaatcatgtcatagc-3'
	fLuc-Not1-R	5'-gctatgacatgattacggcggccgctttttttttttttttttttttttttttgggg-3'

Extended Data Table 2 | Primers used in the generation of EEEV mutant viruses

Virus	Primer Name	Sequence
11337	EEEV11337-F	5′-gacattaacatcttgtcaaccggcagcgcataatgctgtcttttatatc-3′
	EEEV11337-R	5′-gatataaaagacagcattatgcgctgccggttgacaagatgttaatgtc-3′
142del	EEEV-Del-1-2-F	5'-catagacattaacatcttgggcagtgtataaggcttcaccctagttcgatgtacttccg-3'
	EEEV-Del-1-2-R	5'-cggaagtacatcgaactagggtgaagccttatacactgcccaagatgttaatgtctatg-3'
	EEEV-Del-3-4-F	5'-ctttataatcaggcataattgggtaatataccgcctggcagcgcataatgctgtc-3'
	EEEV-Del-3-4-R	5'-gacagcattatgcgctgccaggcggtatattacccaattatgcctgattataaag-3'
142pm	ΔmiR-142-1-F	5′-taacatcttgtcaaccacataactcaagaggcagtgta-3′
	ΔmiR-142-1-R	5′-attgtagaacagttggtgtattgagttctccgtcacat-3′
	ΔmiR-142-2-F	5′-taaggctgtcttactaaactcaagattcaccctag-3′
	ΔmiR-142-2-R	5′-ctagggtgaatcttgagtttagtaagacagcctta-3′
	ΔmiR-142-3-F	5′-gcataattgccgtatatacaattactcaagaggtaatataccgcctcttataaa-3′
	ΔmiR-142-3-R	5′-tttataagaggcggtatattacctcttgagtaattgtatatacggcaattatgc-3′
	ΔmiR-142-4-F	5′-ataccgcctcttataaactcaagaggcagcgc-3'
	ΔmiR-142-4-R	5′-gcgctgcctcttgagtttataagaggcggtat-3′